

Metalimnetic oxygen minimum and the presence of *Planktothrix rubescens* in a low-nutrient drinking water reservoir

Author

Wentzky, Valerie C, Frassl, Marieke A, Rinke, Karsten, Boehrer, Bertram

Published

2019

Journal Title

Water Research

Version

Accepted Manuscript (AM)

DOI

[10.1016/j.watres.2018.10.047](https://doi.org/10.1016/j.watres.2018.10.047)

Rights statement

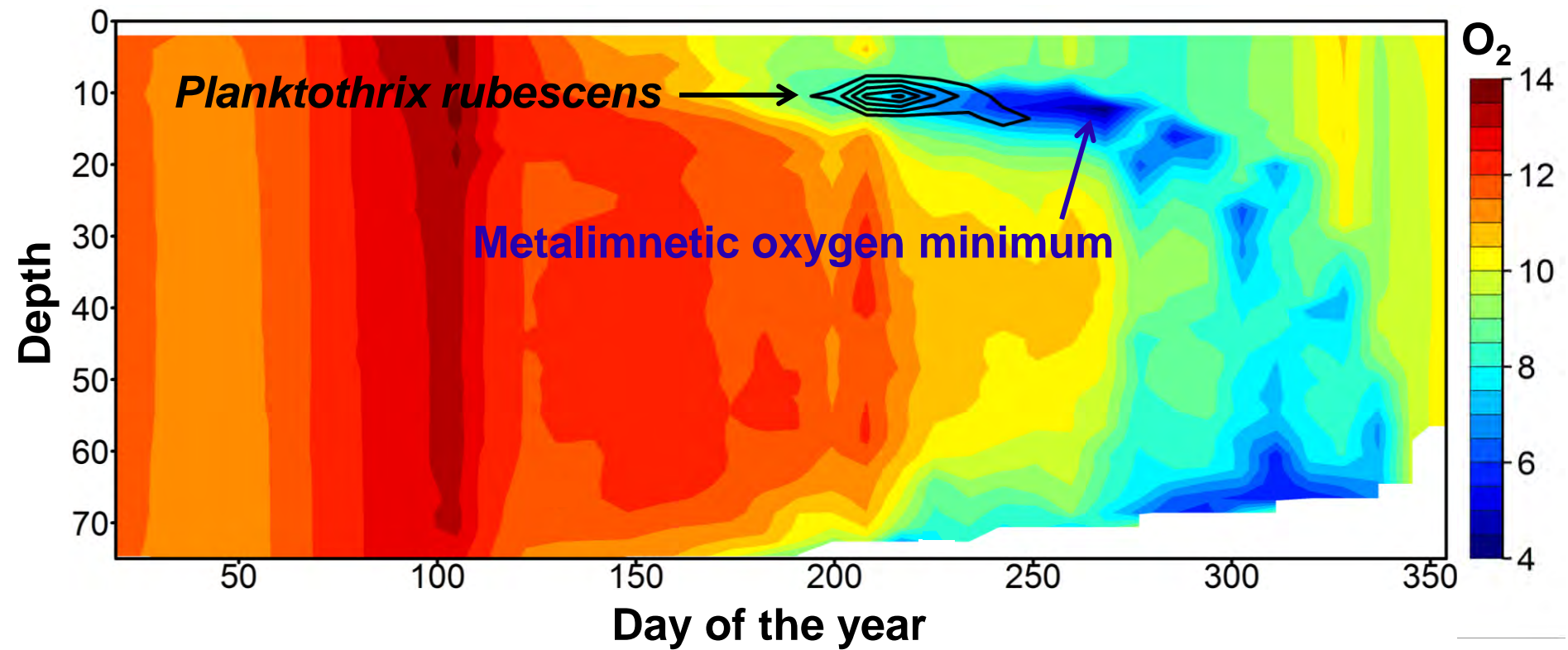
© 2019 Elsevier. Licensed under the Creative Commons Attribution-NonCommercial-NoDerivatives 4.0 International Licence which permits unrestricted, non-commercial use, distribution and reproduction in any medium, providing that the work is properly cited.

Downloaded from

<http://hdl.handle.net/10072/383181>

Griffith Research Online

<https://research-repository.griffith.edu.au>



Metalimnetic oxygen minimum and the presence of *Planktothrix rubescens* in a low-nutrient drinking water reservoir

Valerie C. Wentzky^{a*}, Marieke A. Frassl^{a,b}, Karsten Rinke^a, Bertram Boehrer^a

5 ^a Helmholtz Centre for Environmental Research–UFZ, Brueckstrasse 3a, D-39114

Magdeburg, Germany

^b Australian Rivers Institute, Griffith University, 170 Kessels Rd, Nathan, Queensland

4111, Australia

10 *Corresponding author: valerie.wentzky@ufz.de, phone +49 391 810 9440

Abstract

15

Dissolved oxygen is a key player in water quality. Stratified water bodies show distinct vertical patterns of oxygen concentration, which can originate from physical, chemical or biological processes. We observed a pronounced metalimnetic oxygen minimum in the low-nutrient Rappbode Reservoir, Germany. Contrary to the situation in the hypolimnion, measurements of lateral gradients excluded the sediment contact zone from the major sources of oxygen depletion for the metalimnetic oxygen minimum. Instead, the minimum was the result of locally enhanced oxygen consumption in the open water body. A follow-up monitoring included multiple chlorophyll a fluorescence sensors with high temporal and vertical resolution to detect and document the evolution of phytoplankton. While chlorophyll fluorescence sensors with multiple channels detected a mass development of the phycoerythrin-rich cyanobacterium *Planktothrix rubescens* in the metalimnion, this species was overseen by the commonly used single-channel chlorophyll sensor. The survey indicated that the waning *P. rubescens* fluorescence was responsible for the oxygen minimum in the metalimnion. We hypothesize that pelagic processes, i.e., either oxygen use through decomposition of dead organic material originating from *P. rubescens* or *P. rubescens* extending its respiration beyond its photosynthetic activity, induced the metalimnetic oxygen minimum. The deeper understanding of the oxygen dynamics is mandatory for optimizing reservoir management.

35

40 **Key Words:**

Oxygen depletion, metalimnion, lake stratification, deep chlorophyll maximum, Rappbode

Reservoir, fluorescence sensors

ACCEPTED MANUSCRIPT

1. Introduction

45

Dissolved oxygen is a key variable for nearly all organisms in the aquatic environment. Especially in stratified lakes, vertical transport of dissolved substances is limited, which can result in sharp vertical gradients of oxygen concentration. Usually in direct contact with the atmosphere, the epilimnion shows a gas pressure that is close to equilibrium with the atmosphere, while the hypolimnion has trapped a limited amount of oxygen, which is subjected to depletion over the summer months until the thermal stratification breaks and deep recirculation recharges the hypolimnion with oxygen (e.g., Boehrer and Schultze, 2008).

50

55

In many cases, however, a more complex picture is observed. Especially in the thermocline, where high density gradients restrict the vertical exchange, gradients of dissolved substances are formed and sustained due to small vertical transport. Both metalimnetic oxygen maxima and metalimnetic oxygen minima can be found. Though both features are commonly encountered, oxygen maxima have been dealt with in more detail in the literature (e.g., Wilkinson et al., 2015). Here we concentrate on the case of metalimnetic oxygen minima, which often get attributed to eutrophic lakes (e.g., Lake Arendsee: Boehrer and Schultze, 2008; in general see also Wetzel, 2001) or reservoirs (Zhang et al 2015); however, also lakes of lower trophic state can show metalimnetic oxygen minima (e.g., Joehnk and Umlauf, 2001).

60

65

Metalimnetic maxima can appear as an artefact when trapped water warms and hence saturation levels increase due to lower solubility of oxygen at higher temperatures (e.g., Wilkinson et al., 2015). Alternatively, oxygen maxima can originate from oxygen production by photosynthesising phytoplankton (Parker et al., 1991; Stefan et al., 1995),

70 which form a deep chlorophyll maximum in the metalimnion. Deep chlorophyll maxima
can be observed in many lakes (Leach et al., 2017). In contrast to metalimnetic oxygen
maxima, metalimnetic oxygen minima cannot be the consequence of diffusive heating
from the surface and hence must result from oxygen depletion. When a minimum forms,
the shape of the oxygen profile depends on both: the oxygen depletion at the respective
75 depth as well as vertical transport from the layers above and below (Kreling et al., 2017).

Both, oxygen depletion in the open water and at the sediment surface can be responsible
for the formation of a metalimnetic oxygen minimum. Modelling approaches include one
oxygen depletion rate in the water column and one value for the oxygen depletion rate per
80 sediment surface (e.g., Livingstone and Imboden, 1996; Weber et al., 2017). Often oxygen
consumption by the sediment is considered as the leading part. In addition, advective
processes like inflows with high oxygen demand have been claimed to be important: flood
waters with easily degradable organic material often find their way into the metalimnion of
a stratified water body (as shown by Nix, 1981; DeGray Reservoir, Arkansas USA). As
85 oxygen depletion in a lake is usually attributed to the sediment contact zone, it has been
reasoned that the oxygen minimum can be an effect of oxygen depletion at the side
boundaries, which is advected into the main body of the lake on isopycnal (constant
density) surfaces. The corresponding lake morphometry may be supportive of different
depletion rates (Shapiro, 1960; Wetzel, 2001) due to variable ratios of sediment area to
90 layer volume with depth and varying temperatures with depth.

Despite its low trophic status, a reoccurring metalimnetic oxygen minimum was observed
in the Rappbode Reservoir (see Fig. 7). Hence we planned an investigation of the
metalimnetic oxygen minimum, to find clues about possible reasons. Understanding
95 oxygen depletion is essential for a proper management of reservoirs. Low oxygen

conditions interfere with water quality and can thereby largely increase costs of drinking water treatment. Too low oxygen concentrations are also risky for biota within the lake depending on a sufficient oxygen supply, like fish (Rice, 2013). The Rappbode Reservoir harbours a managed stock of lake trout (*Salmo trutta f. lacustris*), which are sensitive to low oxygen levels and, therefore, concentrations below 4 mg L⁻¹ should be avoided.

To shed light on the causes of the metalimnetic oxygen minimum in the Rappbode Reservoir, we organised our investigation in three distinct steps, over two years:

- (1) The horizontal and vertical variability of the oxygen minimum was studied on one single day in September 2015 to determine the location of the most intense oxygen depletion (possibly the sediment surface?).
- (2) The temporal and spatial evolution of the oxygen in 2016 was documented by measurements of multiparameter profiles of high resolution.
- (3) The ecological evolution was studied by multichannel fluorescence profiles with fine vertical resolution and water samples for identification of organisms with microscopy.

115

120

2. Field Site, Measurements and Methods

The Rappbode Reservoir is located in the Harz Mountains in Northern Germany (coordinates 51°44'N 10°54'E) and is the largest drinking water reservoir in Germany (in terms of volume), providing water to about 1 million people. The catchment is covered by forest and farmland (Friese et al., 2014). The dam has been constructed in the 1950s forming a lake of a complex shape with an 8 km long main channel towards south-west and two side arms facing north and south (Fig. 1). Water enters via three pre-dams, which have been built for the purpose of sediment and nutrient retention (Rinke et al., 2013). The reservoir has a maximum depth of 89 m and a mean depth of 28.6 m. As typical for deep temperate water bodies, the Rappbode Reservoir completely mixes in late autumn and spring. It always stratifies in summer, but only occasionally in winter during the last years, due to the lack of ice cover. Since 1991, phosphorus concentrations have been low enough to expect a mesotrophic to oligotrophic waterbody (on average 0.014 mg L⁻¹ total phosphorus during the last 10 years, Wentzky et al., 2018). More information about the major ion composition and physicochemical properties of Rappbode water can be found in Moreira et al. (2016). Details about dissolved organic carbon composition are given in Tittel et al. (2015) and Morling et al. (2017).

Taking advantage of the morphometric complexity of the reservoir, we measured two transects: longitudinally (L16-L1 in Fig. 1), following the thalweg as closely as possible from the dam wall to the beginning of the backwater, and laterally from one side arm across the main channel towards the steep opposite side wall (T1-T7 in Fig. 1). We used a multiparameter probe (CTD90M Sea and Sun Technology, Trappenkamp, Germany, serial number: 644) with sensors for chlorophyll a fluorescence (Cyclops 7, model number: 2100-000, excitation wavelength 460 nm), temperature (PT100), electrical conductivity,

pressure (for depth) and dissolved oxygen (optical sensor, Rinko III) with a response time of about 2 s. The species *Planktothrix rubescens* is almost invisible for the Cyclops 7
150 sensor with blue excitation, since the fluorescence yield of *P. rubescens* for this sensor's excitation wavelength (460 nm) is very low. The reasons for this low fluorescence yield is low chlorophyll a content in photosystem II and the lack of alternative pigments that absorb light at the applied short wavelengths. The investigation was conducted in late summer (10th September 2015) when the metalimnetic oxygen minimum had enough time
155 to develop, but clearly before any large-scale cooling driven recirculation set in.

We further made use of a regular monitoring programme, in which multiparameter probe profiles (as in Fig. 2) were measured at fortnightly intervals during the entire year 2016 (from 19th January 2016 to 19th December 2016). The multiparameter probe mentioned
160 above was used. Additionally, a multi-channel fluorescence probe (FluoroProbe, bbe moldaenke GmbH, Germany, serial number: 2101) was used to detect phytoplankton and to characterise the algal community. The FluoroProbe measured fluorescence emitted from chlorophyll a in the PS II (at wavelength 685 nm), which was triggered through the excitation at different wavelengths (370, 470, 525, 570, 590 and 610 nm). The signal at
165 370 nm excitation wavelength was used to correct for the fluorescence of dissolved organic matter. The other wavelengths referred to different accessory pigments present in phytoplankton, which allowed discrimination into four algal groups: (1) Green algae (rich in chlorophyll a/b), (2) diatoms/dinoflagellates (containing xanthophyll and chlorophyll c), (3) phycocyanin-rich cyanobacteria and (4) phycoerythrin-rich cyanobacteria and
170 cryptophytes (for more information on the measurement principle we refer to Beutler et al., 2002a and 2002b). We used the probe measurements, and more precisely the signal of the red group (cryptophytes and phycoerythrin-rich cyanobacteria, excitation wavelength 570 nm), for assessing the vertical distribution of the phycoerythrin-rich cyanobacterium

Planktothrix rubescens in the water column (for more information on occurrence of
175 cyanobacteria in general see Carey et al., 2012 and specifically for stratified lakes see
Cuypers et al., 2011).

To get a clearer picture of the short-term dynamics and spatio-temporal distribution
patterns, in the following year (2016), we installed an automatic profiler system (for
180 location of profiler see Fig. 1) with a multiparameter probe (YSI 6820 V2-2 O) including
sensors for dissolved oxygen (YSI 6150), temperature (YSI 6560), and two sensors for
chlorophyll fluorescence: one sensor measuring chlorophyll a fluorescence directly (YSI
6025, excitation wavelength 470 nm) and one measuring chlorophyll fluorescence via
exciting phycocyanin (YSI 6131, excitation wavelengths 565-605 nm). Besides
185 phycoerythrin, *P. rubescens* also contains phycocyanin and hence could also be detected
by the phycocyanin sensor. The profiler covered the upper 26 m of the water column with
depth-intervals of 0.25 m between 0-20 m and 0.5 m from 20-26 m. Profiles were
measured at intervals of three hours. Operation began on 4th August 2016 and ran until 9th
November 2016.

190

For microscopic species determination, phytoplankton samples were preserved with
Lugol's solution, concentrated using the sedimentation technique developed by Utermöhl
(1958) and counted under an inverted light microscope. Most phytoplankton taxa were
counted as cells. An exception was filamentous phytoplankton, such as *P. rubescens*,
195 which was counted by measuring the filament length. Biovolumes for each species were
derived from average cell dimension measurements and simple geometric shapes
(Hillebrand et al, 1999). Phytoplankton biovolume was converted to biomass assuming a
specific density of 1.0.

200 To assess the long-term development of oxygen in the Rappbode Reservoir, weekly oxygen profiles were taken between 2009 and 2016. Oxygen concentrations and temperatures were measured with the DS5 multiparameter probe from Hydrolab. (An overview about all probes and sensors used in this study, including information about their characteristics, can be found in Table A1 in the supporting information.)

205

As a stability quantity of stratification, the square buoyancy frequency (N^2) was calculated from CTD90M profiles, using the formula

$$N^2 = -\frac{g}{\rho} \cdot \frac{d\rho}{dz}$$

where density ρ was calculated using a specific formula for the Rappbode Reservoir from Moreira et al. (2016), g was the earth acceleration (9.81 m/s^2) and z was the vertical coordinate. In discrete steps,

210

$$\begin{aligned} N^2 &= -\frac{g}{\rho(z)} \cdot \frac{\rho(z+a) - \rho(z-a)}{(z+a) - (z-a)} \\ &= -\frac{g}{\rho(z)} \cdot \frac{\rho(z+a) - \rho(z-a)}{2a} \end{aligned}$$

where $a \sim 1\text{m}$ was the vertical resolution of the calculation. For other quantities on stability see MacIntyre et al. (2009), Boehrer and Schultze (2009) and Read et al. (2011).

Chlorophyll a fluorescence values obtained by the FluoroProbe and the multi-parameter
 215 CTD90M probe were supplied as $\mu\text{g L}^{-1}$ of chlorophyll by the manufacturer. However, before using the chlorophyll a fluorescence data quantitatively, they were compared with high pressure liquid chromatography (HPLC) measurements to evaluate the accuracy of the probe measurements. Samples for HPLC analysis were taken biweekly at the same sampling dates as the vertical probe profiles. Samples were collected at discrete depths (0,
 220 2.5, 5, 10, 15, 20, 25, 30, 40, 50, 60, 70 m) using an open cylinder water sampler (4.2 L

standard water sampler from Limnos). The total number of water samples used for analysis was 229. For chlorophyll a quantification, 1.5 L of sample water was filtered using glass fibre filters and extracted with 5 mL ethanol and several freezing/thawing cycles. Subsequently 20 μ L of extract was measured by HPLC (for details on method see Van Pinxteren, 2017). For comparison, the probe data were aggregated to the same discrete depth levels as the HPLC samples. To test for relationships between chlorophyll a data obtained by fluorescence sensors (CTD90M and FluoroProbe) and data from HPLC measurements, linear regression analysis was performed: The coefficients of determination (R^2) described the relationship between both variables and indicated the goodness of fit ($R^2=0$: no relationship; $R^2=1$: perfect relationship), while the p-values for the coefficients quantified the statistical significance of this relationship.

For a quantitative estimate of possible oxygen depletion through the deep chlorophyll maximum, we converted the maximum observed chlorophyll a concentration from the FluoroProbe into carbon, using a specific *Planktothrix* C:Chl-a conversion factor of 90 mg C/mg Chl-a (Copetti, 2006). Secondly, we calculated the concentration of possible oxygen depletion by assuming 1 mol C (12 g C) of carbon biomass requires 1 mol O_2 (32 g O_2) for oxidation.

240 3. Results

3.1 Local extension of the metalimnetic oxygen minimum

To localize places of particularly high oxygen depletion, we firstly investigated the horizontal and vertical distribution of the metalimnetic oxygen minimum throughout the Rappbode Reservoir. During our campaign in September 2015, the Rappbode Reservoir showed vertical gradients typical for temperate stratified water bodies (Fig. 2). Below the 10 m thick epilimnion, a density gradient stabilized the water column limiting vertical exchange between the epilimnion and deeper layers. The reservoir showed relatively low conductivity, neutral pH, a chlorophyll a maximum in the epilimnion and a pronounced metalimnetic oxygen minimum.

Surface waters showed oxygen concentrations close to the equilibrium with the atmosphere. On the transversal transect (Fig. 3a), the oxygen curve below 10 m was similar for all profiles. Differences between profiles occurred at deep sites at depths below 20 m. In the longitudinal transect, vertical oxygen profiles varied between different stations (Fig. 3b). The upper edge of the gradient varied by about four meters over the entire length of the reservoir, which could be attributed to uplift and internal waves due to wind stress along the lake (see Bocaniov et al., 2014). All profiles captured a metalimnetic oxygen minimum at depths between 11 and 13 m, oxygen levels of about 55% saturation and documented higher oxygen concentrations in the deep water. Only at station T1, the water depth was too shallow to show the complete structure. Hence the metalimnetic oxygen minimum can be verified throughout the water body at the depth of the maximum density gradient (see Figs. 2c and d).

Below the metalimnetic oxygen minimum, i.e. below 20 to 30 m depth, we found differences of oxygen concentration between profiles: shallower water depths (see shorter profiles) corresponded with lower concentrations of oxygen in the hypolimnion. This fact was indicative of higher oxygen depletion due to a higher sediment area to water volume ratio at the shallow sites, i.e. oxygen depletion imported from the side walls (see e.g., Müller et al., 2012, Dadi et al., 2016). This observation agreed with the approach taken in numerical models, which implement oxygen uptake at the sediment surface as an important contribution for oxygen depletion. Horizontal mixing in the waterbody was obviously not sufficient to remove these oxygen gradients within the hypolimnion. The observation of lower oxygen saturation at stations with a higher sediment influence was visible in both the longitudinal and the lateral transect (Fig. 3).

The depth and extent of the metalimnetic oxygen minimum was identical in all profiles of the lateral transect and also nearly identical in the longitudinal transect from the dam wall (L16) up to at least station L8. Further above, along the thalweg towards the inflow, the water was very shallow and differences between the profiles became visible. In conclusion, there was no indication that oxygen depletion in the metalimnion would vary between locations throughout most of the water body and no horizontal gradients were observable as seen in the hypolimnetic oxygen levels. Hence, the prevailing oxygen depleting process in the metalimnion was the same along the horizontal axes of the water body. As the sediment contact area in the side arm was larger than in the main channel or at the rock wall, the leading process for oxygen uptake could not significantly be connected to the sediment. In conclusion, the measurements indicated that the metalimnetic oxygen minimum in the Rappbode Reservoir was the consequence of pelagic processes.

290

3.2 Temporal evolution of the metalimnetic oxygen minimum

The results of the transect measurements clearly showed that no horizontal gradient was visible in the metalimnetic oxygen minimum. Accordingly, measurements at one single pelagic site were sufficient to investigate the temporal evolution.

Temperature stratification in 2016 was typical for the location (Wentzky et al., 2018). The summer stagnation period started in April after day of the year (DOY) 100 (see contour lines Figs. 4a-c) and lasted until December. During summer, the major temperature gradient was located at around 10 m depth, which deepened slightly over time. Phytoplankton (chlorophyll fluorescence, Figs. 4a and b) increased after thermal stratification had started. Later in summer, a strong phytoplankton peak occurred in the metalimnion, as indicated by the chlorophyll fluorescence measured by the multi-channel FluoroProbe (Fig. 4b). This deep phytoplankton peak was not visible in the chlorophyll a profile measured by the Cyclops 7 sensor of the CTD90M probe, which used only one single excitation wavelength and cannot detect phycoerythrin-rich cyanobacteria like *Planktothrix* (Fig. 4a).

Specific *in situ* fluorescence measurements of the “red channel” of the FluoroProbe (representing phycoerythrin-rich cyanobacteria and cryptophytes) indicated the development of the phycoerythrin-rich cyanobacterium *P. rubescens* in the metalimnion (Fig. 4c). This fluorescence signal was present from DOY 200 (18th July) to DOY 230 (17th August) and faded out over further 40 days (until DOY 270). Likewise, phycocyanin fluorescence was recorded at the thermocline depth and hardly ever at other depths or other times (Fig. 5c). Microscopic inspection of the phytoplankton confirmed the occurrence and dominance of *P. rubescens* at the respective depths (Fig. A1 supporting information). In addition, the cyanobacteria *Oscillatoria limnetica* and *Limnothrix redekei*, which contain

phycocyanin but not phycoerythrin, were observed in the metalimnion, but at very low abundances. In conclusion, the signal of the “red channel” of the FluoroProbe and the
320 phycocyanin fluorescence measured by the automatic profiler system could mainly be attributed to *P. rubescens*.

Oxygen concentrations were high during deep recirculation in winter and early spring due to cold temperatures and mixis of re-oxygenated water from the surface (Fig. 4d). In the
325 epilimnion, oxygen concentrations during summer dropped due to higher temperatures and hence lower solubility. In the hypolimnion, oxygen was confined and subject to gradual depletion. As in the previous year, a clear minimum appeared at the thermocline after DOY 230 (17th August) and ended when the recirculation included the oxygen depleted layers into the surface mixed layer. Minimal oxygen levels in the metalimnion reached down to 4
330 mg L⁻¹ around DOY 270 (26th September). Towards the end of the stratification period, low oxygen concentrations were found at the lake bed until the deep recirculation also removed this minimum. In some summer profiles, we observed small distinct local oxygen maxima of up to 0.5 m thickness at the upper edge of the metalimnion, directly above the oxygen minimum (Fig. A2 supporting information). These peaks were an indicator for
335 oxygen production by photosynthetic organisms. Due to the small extent of the peaks, they were not visible in the contour plots.

The formation of the metalimnetic oxygen minimum coincided with the breakdown of the metalimnetic *P. rubescens* population (Fig. 4d and Fig. A1 in supporting information).
340 Moreover, the layer thickness of the oxygen minimum resembled the thickness of the *Planktothrix* layer before and looked like the continuation of the previous feature.

The high-resolution data from the automatic profiler confirmed the upper edge of the metalimnetic oxygen minimum as the lower boundary of the epilimnion (Figs. 5a and d).

345 The oxygen minimum was clearly terminated by the gradual inclusion of the oxygen depleted layer into the epilimnion. The high resolution data also revealed additional features, such as elevated chlorophyll a fluorescence at the time and depth where phycocyanin occurred (Figs. 5b and c).

350 The disappearance of phycocyanin (mainly representing *P. rubescens*) coincided with the strong oxygen depletion, which stopped at a saturation level of about 40% (or 4 mg O₂ L⁻¹) (Figs. 5c and d). Since the stratification persisted for longer, oxygen concentrations could have dropped further, if oxygen depletion had continued. A downward track of phycocyanin indicated that layers were drawn down due to shrinking hypolimnetic volume
355 as a consequence of withdrawal through the bottom outlet. Notably, the oxygen minimum followed this downward trend.

3.3. Comparison of chlorophyll a quantification methods based on fluorescence with HPLC

360 Chlorophyll a values obtained by the CTD90M probe and FluoroProbe during the monitoring in 2016 were in good agreement with HPLC measurements from discrete sampling (Fig. 6). The fit of the correlation with HPLC was higher for the FluoroProbe ($R^2=0.78$, $p<0.001$) than for the CTD90M ($R^2=0.63$, $p<0.001$). The FluoroProbe and the CTD90M probe were also significantly correlated ($R^2=0.62$, $p<0.001$). As a result of the
365 good correlation between chlorophyll a fluorescence of the probes and chlorophyll a concentrations measured by HPLC, the values of the FluoroProbe were later used for a quantitative estimate on phytoplankton carbon biomass.

3.4 Calculation of potential oxygen depletion from available phytoplankton carbon

370 *biomass*

Our calculations showed that 3.1 mg O₂ L⁻¹ oxygen could be depleted from the available phytoplankton carbon biomass in the metalimnion (12.79 µg chl-a L⁻¹ or respectively 1.15 mg C L⁻¹). In 2016, we observed an oxygen depletion of about 5 mg O₂ L⁻¹ in the Rappbode Reservoir (Fig. 4a). Since the calculated and the observed oxygen depletion
375 were in a similar range, the *Planktothrix* biomass in the metalimnion could be connected to the metalimnetic oxygen minimum formation.

4. Discussion

380 A pronounced metalimnetic oxygen minimum, which reached down to only 40% saturation level, was documented in the meso- to oligotrophic Rappbode Reservoir. The distinctiveness of the metalimnetic minimum was surprising, given the low trophic state of the reservoir and the low phytoplankton abundance. The oxygen depleted water volume showed a sharp upper edge to the epilimnion and extended about 5 m into the stratified
385 waterbody below. The oxygen minimum endured from the middle of August, when a population of *P. rubescens* disappeared at the same depth, to the end of October, when deep recirculation removed the metalimnion by inclusion into the epilimnion.

The small horizontal variability observed in September 2015 (Fig. 3) indicated that the
390 forming process was not significantly connected to side wall effects, such as oxygen depletion at the sediment surface, inflows or side wall mixing providing water that could have intruded the metalimnion. The oxygen depletion had to be mainly attributed to depletion in the open water body. Hence the further investigation focused on finding reasons for oxygen depletion in the pelagial.

395

There was evidence for a connection of the metalimnetic oxygen minimum to the phycocyanin fluorescence maximum measured by the automatic profiler (as well as to the signal of the “red channel” of the FluoroProbe) and thus organisms related to this fluorescence (Figs. 4d and 5c-d): firstly the oxygen minimum formed in the same water layers, secondly the oxygen depletion started with the disappearance of the phycocyanin (and the signal of the “red channel” of the FluoroProbe respectively) and thirdly the depletion stopped at 40% of oxygen saturation. Hence there seemed to be a limited reservoir of oxygen demand. Phycocyanin fluorescence and the signal detected by the “red channel” of the FluoroProbe could be related to a *P. rubescens* mass development, which was microscopically confirmed in the Rappbode Reservoir at the respective depths. Most likely, the oxygen depletion was related to the discontinuation of photosynthetic activity of the *Planktothrix* population.

A metalimnetic *P. rubescens* maximum has also been observed in other lakes (Walsby & Schanz, 2002; Cuypers, 2011). *P. rubescens* populations commonly form at this depth, since gas vesicles allow regulating their position within the depth of optimal growth conditions (Walsby et al., 2004). Their preference for the metalimnion is due to physiological traits that differ from those of other bloom forming species: *P. rubescens* favours low temperatures (Dokulil & Teubner, 2000; Holland & Walsby, 2008) and is adapted to low light conditions (Walsby & Schanz, 2002; Walsby & Jüttner, 2006). Its ability to use organic compounds as a carbon source under extremely low irradiances (photoheterotrophy) allows for survival and even slow growth in the metalimnion (Zotina et al., 2003). As in the Rappbode Reservoir, *P. rubescens* has been found to be a dominant species in the metalimnion even under low nutrient conditions (Steinberg & Hartmann, 1988; Posch, 2012).

While the *P. rubescens* peak was detected by the multi-channel FluoroProbe (*excitation wavelengths 470, 525, 570, 590 and 610 nm*, Fig. 4b), it was not captured by the single-channel chlorophyll a fluorescence measurements of the Cyclops-7 sensor of the CTD90M probe (excitation wavelength 460 nm, Fig. 4a) and chlorophyll a fluorescence YSI sensor of the automatic profiler (excitation wavelength 470 nm, Fig. 5b), which are sensor types commonly used for lake monitoring to estimate phytoplankton biomass (Brentrup et al., 2016). Given the importance of phycoerythrin-rich species such as *P. rubescens* for biogeochemical processes, important information might be missed by using chlorophyll a fluorescence sensors with only one single excitation wavelength to quantify chlorophyll a or phytoplankton biomass. This finding agrees well with other studies showing that chlorophyll a concentration and phytoplankton biovolume were better estimated by the FluoroProbe than by chlorophyll sensors measuring only at a single wavelength, especially in case of cyanobacterial blooms (e.g., Gregor & Marsálek, 2004; Catherine et al., 2012). Given the fact that *P. rubescens* is almost invisible for chlorophyll fluorescence sensors based on blue excitation implies that the occurrence of this highly relevant cyanobacteria can be overlooked in monitoring campaigns. Hence, for a more complete picture of the organisms the use of fluorescence sensors based on multiple wavelengths instead of single-wavelength sensors is recommended. This is particularly important when microscopic cell counts are not conducted and phytoplankton monitoring is entirely based on fluorescence measurements.

Moreover the FluoroProbe had been shown to strongly correlate with the standard ISO method for chlorophyll a quantification ($r^2 = 0.97$, $p < 0.05$, Gregor & Marsálek, 2004) as well as with phytoplankton biovolume obtained by microscopic analysis ($r^2 = 0.89$, p -value < 0.001 , Catherine et al., 2012). This was valid also for cyanobacteria dominated waters:

for instance, Leboulanger (2002) found that *P. rubescens* cell counts from discrete sampling were closely correlated with data obtained by the FluoroProbe ($r^2 = 0.89$, $p < 0.01$, Leboulanger, 2002). Also during the monitoring in 2016 in the Rappbode Reservoir chlorophyll a fluorescence measured by the FluoroProbe compared well with chlorophyll a concentrations determined by the HPLC method ($R^2=0.78$, $p<0.001$, Fig. 6b). In conclusion, we used chlorophyll a fluorescence measurements from the FluoroProbe to get a rough quantitative estimate of phytoplankton carbon biomass. Using this approximation of phytoplankton carbon biomass, our calculations showed that it could deplete approximately $3.1 \text{ mg O}_2 \text{ L}^{-1}$. Considering that this value was just a rough estimate, it compared rather well with the observed oxygen depletion in the metalimnion of $5 \text{ mg O}_2 \text{ L}^{-1}$. Nevertheless, a reason for the discrepancy between calculated and observed value might lie in the fact that the peak of the *Planktothrix* biomass was not recorded by our biweekly monitoring programme.

460

The oxygen minimum in the metalimnion in late summer was a reoccurring feature in the Rappbode Reservoir (Fig. 7). Phytoplankton count data verified the presence of *P. rubescens* during summer at the thermocline since 2009, usually with a peak at a depth around 10 m. The occurrence of *P. rubescens* in previous years and the simultaneous observation of a metalimnetic oxygen minimum supported our hypothesis, that both features were connected.

465

Both features, the colonization by *P. rubescens* and the persistence of a metalimnetic oxygen minimum were connected to the presence of density stratification: a) for *P. rubescens* to allow for depth control by buoyancy, b) for the metalimnetic oxygen minimum to limit the diffusive exchange with neighbouring layers at higher oxygen concentration. Hence we displayed both features within the stratification (Fig. 8), where

470

we calculated the square buoyancy frequency (N^2) from CTD90M profiles. Both, the *P. rubescens* fluorescence and the oxygen minimum followed the depths of high density
475 gradients.

Prior to this study, the connection between metalimnetic *P. rubescens* mass developments and metalimnetic oxygen depletion had not been studied nor documented in similar detail. However, we found hints in the literature that also in other lakes low metalimnetic oxygen
480 levels occurred simultaneously with the predominance of *P. rubescens*, supporting our hypothesis of a causal relationship between both. For example, in Lake Zürich (Switzerland), known for its recurrent mass developments of *P. rubescens* in summer (Micheletti et al., 1998), a metalimnetic oxygen minimum developed subsequent to a *Planktothrix* bloom in the metalimnion (Van den Wyngaer et al., 2011). Moreover, profile
485 measurements conducted in Crooked Lake (USA) in the summer of 1979 showed a metalimnetic *Planktothrix* peak accompanied by a decrease in oxygen (Konopka, 1980). In Lake Ammersee (Germany) a gradual depletion of oxygen to very low levels was reported, slightly below a *Planktothrix* peak (Ernst et al., 2001; Hofmann and Peeters, 2013).

490 We could think of three reasonable cases that produced an oxygen depletion with the disappearance of photosynthetic activity in the metalimnion: (1) *Planktothrix rubescens* died and microbial degradation of its biomass required oxygen (2) *P. rubescens* perpetuated respiration longer than photosynthetic activity (3) heterotrophic organisms requiring oxygen for respiration (Shapiro, 1960; Raateoja et al., 2010), which was
495 disguised while *Planktothrix* was photosynthetically active in the metalimnion. However, firstly the quantitative estimate of possible oxygen depletion through *Planktothrix*, as well as secondly the local confinement of the oxygen depletion to the same depths as the deep

chlorophyll maximum and thirdly the termination of oxygen depletion at 40% saturation indicate that process (3) is probably of subordinate importance.

500

Considering that mass developments in the metalimnion of *P. rubescens* were favoured by lake warming (Posch, 2012; Yankova, 2017), metalimnetic oxygen minima might increase simultaneously with *Planktothrix* blooms during the next decades, causing severe problems for water quality. Given the importance of oxygen for water quality, the connection
505 between *P. rubescens* in the metalimnion and oxygen depletion should be studied further and analysed also in other lakes.

5. Conclusions

- A reoccurring metalimnetic oxygen minimum was observed in the low nutrient
510 Rappbode Reservoir (Germany) during late summer. It was characterized by a sharp edge towards the epilimnion and a thickness of about 5 m.
- Oxygen depletion in the metalimnion was a consequence of processes occurring in the pelagic water and was not imported from the sediment on the side walls nor by inflows.
- The emergence of the metalimnetic oxygen minimum was connected to the
515 disappearance of a *Planktothrix rubescens* population in the metalimnion.
- The available phytoplankton carbon biomass could suffice to deplete oxygen in the observed range. This suggested that biological activity induced by the end of a *Planktothrix* mass development was an essential factor in forming the oxygen
520 minimum in the Rappbode Reservoir.
- The presence of *P. rubescens* was responsible for the later appearance of the metalimnetic oxygen minimum either through bacterial decomposition of dead *P. rubescens* cells, or respiration of *P. rubescens* beyond their photosynthetic activity.

The presented data showed no evidence for significant oxygen consumption in the
525 metalimnion from sources other than the deep chlorophyll maximum.

Acknowledgements

Many thanks to Karsten Rahn and Martin Wieprecht for preparing field equipment and
acquiring the fortnightly profiles, many thanks to Burkhard Kuehn for deploying the
530 automatic profiling station on the Rappbode Reservoir, thanks to Kerstin Lerche for
analysing chlorophyll a via HPLC, thanks to Philipp Keller for preparing the bathymetric
map, and thanks to the participants of a teaching excursion on “physical limnology” of the
Heidelberg University for the longitudinal and lateral transect. We also thank the water
supply works Wasserwerk Wienrode (especially Jan Donner) for sharing phytoplankton
535 counts and profile data with us. This research was supported by grants JA 2146/2-1 and RI
2040/2-1 from the German Research Foundation (DFG) within the priority program 1704
“DynaTrait” as well as the project “Managing Water Resources for Urban Catchments”
(grant number 02WCL1337A) by the German Federal Ministry of Education and Research
(BMBF).

540

545

550 **References:**

Beutler, M., Wiltshire, K. H., Lüring, C., Moldaenke, C., Lohse, D., 2002a. Fluorometric depth-profiling of chlorophyll corrected for yellow substances. *Aquaculture Environment and Marine Phytoplankton* 34 (ed. G. Arzul), 231-238.

Beutler, M., Wiltshire, K. H., Meyer, B., Moldaenke, C., Lüring, C., Meyerhöfer, M.,
555 Hansen, U.-P., Dau, H., 2002b. A fluorometric method for the differentiation of algal populations in vivo and in situ. *Photosynthesis Research* 72(1), 39-53.

Bocaniov, S.A., Ullmann, C., Rinke, K., Lamb, K.G., Boehrer, B., 2014. Internal waves and mixing in a stratified reservoir: insights from three-dimensional modeling. *Limnologica* 49 , 52 – 67.

560 Boehrer, B., Schultze, M., 2008. Stratification of lakes. *Reviews of Geophysics* 46(2).

Boehrer, B., Schultze, M., 2009. Density stratification and stability. In: Likens, G.E. (ed.) *Encyclopedia of Inland Waters*, Academic Press, Amsterdam, 583-593.

Brentrup, Jennifer A., Williamson, C.E., Colom-Montero, W., Eckert, W., de Eyto, E.,
Grossart, H.P., Huot, Y., Isles, P.D.F., Knoll, L.B., Leach, T.H., McBride, C.G., Pierson, d.,
565 Pomati, F., Read, J.S., Rose, C.K., Samal, N.R., Staehr, P.A., Winslow, L.A., 2016. The potential of high-frequency profiling to assess vertical and seasonal patterns of phytoplankton dynamics in lakes: an extension of the Plankton Ecology Group (PEG) model. *Inland Waters* 6(4), 565-580.

Catherine A., Escoffier N., Belhocine A., Nasri A.B., Hamlaoui S., Yepremian C.; Bernard
570 C., Troussellier M., 2012. On the use of the FluoroProbe, a phytoplankton quantification

method based on fluorescence excitation spectra for large-scale surveys of lakes and reservoirs. *Water Research* 46(6), 1771-1784.

Carey, C.C., Ibelings, B.W., Hoffmann, E.P., Hamilton, D.P., Brookes, J.B., 2012. Eco-physiological adaptations that favour freshwater cyanobacteria in a changing climate.

575 *Water Research* 46(5), 1394-1407.

Copetti, D., Tartari, G., Morabito, G., Oggiono, A., Legnani, E., Imberger, J., 2006. A biogeochemical model of Lake Pusiano (North Italy) and its use in the predictability of phytoplankton blooms: first preliminary results. *Journal of Limnology* 65(1), 59-64.

580 Cuypers, Y., Vinçon-Leite, B., Groleau, A., Tassin, B., & Humbert, J. F., 2011. Impact of internal waves on the spatial distribution of *Planktothrix rubescens* (cyanobacteria) in an alpine lake. *The ISME Journal* 5, 580-589.

Dadi, T., Friese, K., Wendt-Potthoff, K., Koschorreck, M., 2016. Benthic dissolved organic carbon fluxes in a drinking water reservoir. *Limnology and Oceanography* 61(2), 445-459.

585 Dokulil, M. T., Teubner, K., 2000. Cyanobacterial dominance in lakes. *Hydrobiologia* 438, 1-12.

Ernst, B., Hitzfeld, B., Dietrich, D., 2001. Presence of *Planktothrix* sp. and cyanobacterial toxins in Lake Ammersee, Germany and their impact on whitefish (*Coregonus lavaretus* L.). *Environmental Toxicology* 16(6), 483-488.

590 Friese, K., Schultze, M., Bohrer, B., Büttner, O., Herzsprung, P., Koschorreck, M., Kuehn, B., Rönicke, H., Tittel, J., Wendt-Potthoff, K., Wollschläger, U., Dietze, M., Rinke, K., 2014. Ecological response of two hydro-morphological similar pre-dams to contrasting land-use in the Rappbode reservoir system (Germany). *International Review of Hydrobiology* 99, 335-349.

© Geobasis-De / Lvermgeo Lsa., 2016. <https://www.lvermgeo.sachsen->

595 [anhalt.de/de/download/Geotopographie/main.htm](https://www.lvermgeo.sachsen-anhalt.de/de/download/Geotopographie/main.htm)

Gregor, J., Marsálek, B., 2004. Freshwater phytoplankton quantification by chlorophyll a: a comparative study of in vitro, in vivo and in situ methods. *Water Research* 38, 517-522.

Hillebrand, H., Dürselen, C. D., Kirschtel, D., Pollinger, U., & Zohary, T., 1999.

Biovolume calculation for pelagic and benthic microalgae. *Journal of Phycology* 35, 403–

600 424.

Hofmann, H., Peeters, F., 2013. In-situ optical and acoustical measurements of the buoyant cyanobacterium *P. rubescens*: Spatial and temporal distribution patterns. *PloS One*, 8(11), e80913.

Holland, D. P., Walsby, A. E., 2008. Viability of the cyanobacterium *Planktothrix*

605 *rubescens* in the cold and dark, related to over-winter survival and summer recruitment in Lake Zurich. *European Journal of Phycology* 43(2), 179–184.

Joehnk, K.D., Umlauf, L., 2001. Modelling the metalimnetic oxygen minimum in a medium sized alpine lake. *Ecological Modelling* 136 (1), 67-80.

Konopka, A., 1980. Physiological changes within a metalimnetic layer of *Oscillatoria*

610 *rubescens*. *Applied and environmental microbiology* 40(3), 681-684.

Kreling, J., Bravidor, J., Engelhardt, C., Hupfer, M., Koschorreck, M., Lorke, A., 2017.

The importance of physical transport and oxygen consumption for the development of a metalimnetic oxygen minimum in a lake. *Limnology and Oceanography* 62(1), 348-363.

Leach, T. H., Beisner, B. E., Carey, C. C., Pernica, P., Rose, K. C., Huot, Y.; Brentrup, J.

615 A.; Domaizon, I., Grossart, H.P., Ibelings, B. W., Jacquet, S., Kelly, P. T.; Rusak, J. A., Stockwell, J. D., Straile, D., Verburg, P., 2017. Patterns and drivers of deep chlorophyll

maxima structure in 100 lakes: The relative importance of light and thermal stratification.

Limnology and Oceanography 63(2), 628-646.

Leboulanger C., Dorigo U., Jacquet S., Le Berre B., Paolini G., Humbert J.-F., 2002.

620 Application of a submersible spectrofluorometer for rapid monitoring of freshwater
cyanobacterial blooms: a case study. Aquatic Microbial Ecology 30(1), 83-89.

Livingstone, D.M., Imboden, D.M., 1996. The prediction of hypolimnetic oxygen profiles:
a plea for a deductive approach. Canadian Journal of Fisheries and Aquatic Sciences 53(4),
924-932.

625 MacIntyre S., Fram J.P., Kushner P.J., Bettez N.D., O'Brien W.J., Hobbie J.E., Kling
G.W., 2009. Climate-related variations in mixing dynamics in an Alaskan arctic lake.
Limnology and Oceanography 54(6), 2401-2417.

Micheletti, S., Schanz, F., Walsby, A.E., 1998. The daily integral of photosynthesis by
Planktothrix rubescens during summer stratification and autumnal mixing in Lake Zürich.

630 The New Phytologist 139(2), 233-246.

Moreira, S., Schultze, M., Rahn, K., Boehrer, B., 2016. A practical approach to lake water
density from electrical conductivity and temperature. Hydrology and Earth System
Sciences 20(7), 2975-2986.

Morling, K., Herzsprung, P., Kamjunke, N., 2017. Discharge determines production of,
635 decomposition of and quality changes in dissolved organic carbon in pre-dams of drinking
water reservoirs. Science of The Total Environment 577, 329-339.

Müller, B., Bryant, L.D., Matzinger, A., Wüest, A., 2012. Hypolimnetic oxygen depletion
in eutrophic lakes. Environmental Science and Technology 46(18), 9964-9971.

Nix, J., 1981. Contribution of hypolimnetic water on metalimnetic dissolved oxygen
640 minima in a reservoir. Water Resources Research 17(2), 329-332.

- Parker, B. C., Wenkert, L. J., Parson, M. J., 1991. Cause of the metalimnetic oxygen maximum in Mountain Lake, Virginia. *Journal of Freshwater Ecology* 6(3), 293–303.
- Posch, T., Köster O., Salcher M.M., Pernthaler J., 2012. Harmful filamentous cyanobacteria favored by reduced water turnover with lake warming. *Nature Climate Change* 2(11), 809-813.
- 645 Raateoja, M., Kuosa, H., Flinkman, J., Pääkkönen, J. P., Perttilä, M., 2010. Late summer metalimnetic oxygen minimum zone in the northern Baltic Sea. *Journal of Marine Systems* 80, 1–7.
- Read J.S., Hamilton, D.P., Jones, I.D., Muraoka, K., Winslow, L.A., Kroiss, R., Wu, C.H., Gaiser, E., 2011. Derivation of lake mixing and stratification indices from high-resolution lake buoy data. *Environmental Modelling and Software* 26(11), 1325-1336.
- 650 Rinke, K., Kuehn, B., Bocaniov, S., Wendt-Potthoff, K., Büttner, O., Tittel, J., Schultze, M., Herzsprung, P., Rönicke, H., Rink, K., Rinke, K., Dietze, M., Matthes, M., Paul, L., Friese, K., 2013. Reservoirs as sentinels of catchments: The Rappbode Reservoir Observatory (Harz Mountains, Germany). *Environmental Earth Sciences* 69(2), 523–536.
- Rice, J. A., Thompson, J. S., Sykes, J. A., & Waters, C. T., 2013. The role of metalimnetic hypoxia in striped bass summer kills: consequences and management implications. *American Fisheries Society Symposium* 80.
- Shapiro, J., 1960. The cause of a metalimnetic minimum of dissolved oxygen. *Limnology and Oceanography* 5(2), 216–227.
- 660 Stefan, H. G., Fang, X., Wright, D., Eaton, J. G., McCormick, J. H., 1995. Simulation of dissolved oxygen profiles in a transparent, dimictic lake. *Limnology and Oceanography* 40(1), 105–118.

- Steinberg, C. E., Hartmann, H.M., 1988. Planktonic bloom-forming Cyanobacteria and the
665 eutrophication of lakes and rivers. *Freshwater Biology* 20(2), 279–287.
- Tittel, J., Müller, C., Schultze, M., Musolff, A., Knöller, K., 2015. Fluvial radiocarbon and
its temporal variability during contrasting hydrological conditions. *Biogeochemistry* 126,
57-69.
- Utermöhl, H., 1958. Zur Vervollkommnung der quantitativen Phytoplankton-Methodik.
670 *Mitteilungen der Internationale Vereinigung für theoretische und angewandte Limnologie*
9(1), 1-38.
- Van Pinxteren, M., Barthel, S., Fomba, K. W., Müller, K., Von Tümpling, W., Herrmann,
H., 2017. The influence of environmental drivers on the enrichment of organic carbon in
the sea surface microlayer and in submicron aerosol particles—measurements from the
675 Atlantic Ocean. *Elementa: Science of the Anthropocene* 5(35).
- Van den Wyngaert, S., Salcher, M. M., Pernthaler, J., Zeder, M., Posch, T., 2011.
Quantitative dominance of seasonally persistent filamentous cyanobacteria (*Planktothrix*
rubescens) in the microbial assemblages of a temperate lake. *Limnology and*
Oceanography 56(1), 97-109.
- 680 Walsby, A.E., Schanz, F., 2002. Light-dependent growth rate determines changes in the
population of *Planktothrix rubescens* over the annual cycle in Lake Zürich, Switzerland.
New Phytologist 154(3), 671–687.
- Walsby, A.E., Ng, G., Dunn, C., Davis, P.A., 2004. Comparison of the depth where
Planktothrix rubescens stratifies and the depth where the daily insolation supports its
685 neutral buoyancy. *New Phytologist* 162(1), 133–145.
- Walsby, A. E., Jüttner, F., 2006. The uptake of amino acids by the cyanobacterium
Planktothrix rubescens is stimulated by light at low irradiances. *FEMS Microbiology*
Ecology 58(1), 14–22.

- Weber, M., Rinke, K., Hipsey, M.R., Boehrer, B., 2017. Optimizing withdrawal from
690 drinking water reservoirs to reduce downstream temperature pollution and reservoir
hypoxia. *Journal of Environmental Management* 197, 96-105.
- Wentzky, V.C., Tittel, J., Jäger, C.G., Rinke, K., 2018. Mechanisms preventing a decrease
in phytoplankton biomass after phosphorus reductions in a German drinking water
reservoir –results from more than 50 years of observation. *Freshwater Biology*, 1-14.
- 695 Wetzel, R.G., 2001. *Limnology: lake and river ecosystems*, 3rd ed., Academic Press.
- Wilkinson, G.M., Cole, J.J., Pace, M.L., Johnson, R.A., Kleinmans, M.J., 2015. Physical
and biological contributions to metalimnetic oxygen maxima in lakes. *Limnology and
Oceanography* 60(1), 242-251.
- Zhang, Y., Wu, Z., Liu, M.; He, J., Shi, K., Zhou, Y., Wang, M. & Liu, X., 2015.
700 Dissolved oxygen stratification and response to thermal structure and long-term climate
change in a large and deep subtropical reservoir (Lake Qiandaohu, China). *Water Research*
75, 249-258.
- Yankova, Y., Neuenschwander, S., Köster, O., & Posch, T., 2017. Abrupt stop of deep
water turnover with lake warming: Drastic consequences for algal primary producers.
705 *Scientific Reports* 7(1), 13770.
- Zotina, T., Köster, O., Jüttner, F., 2003. Photoheterotrophy and light-dependent uptake of
organic and organic nitrogenous compounds by *Planktothrix rubescens* under low
irradiance. *Freshwater Biology* 48(10), 1859–1872.

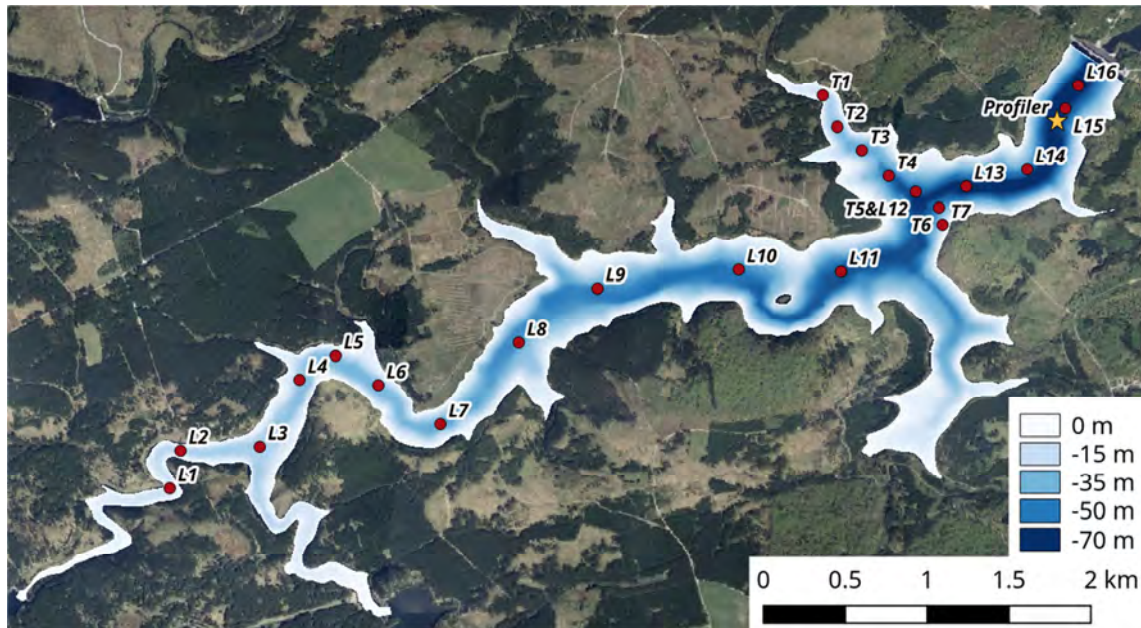


Figure 1: Bathymetric map of the Rappbode Reservoir with sampling stations. Measuring stations L1-L16 belong to the longitudinal transect, while measuring stations T1-T7 belong to the transversal transect. The location of the automatic profiler is indicated by the star. Geologic data were taken from © GeoBasis-DE / LVermGeo LSA (2016).

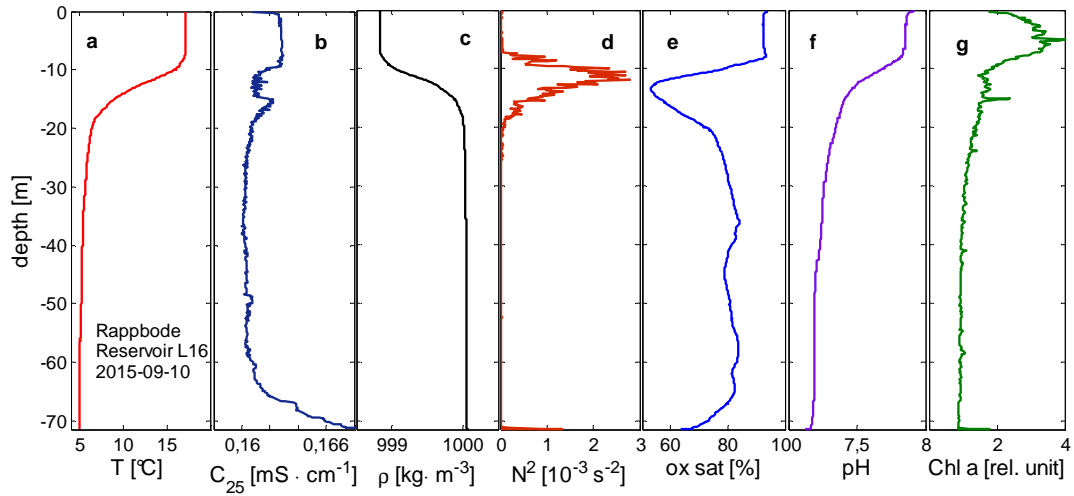


Figure 2: Profiles of (a) temperature, (b) electrical conductivity C_{25} , (c) density, (d) squared buoyancy frequency (calculated), (e) oxygen saturation, (f) pH and (g) fluorescence of chlorophyll a in the Rappbode Reservoir on 10th September 2015 measured at the deep sampling location L16 close to the dam wall (see Fig. 1).

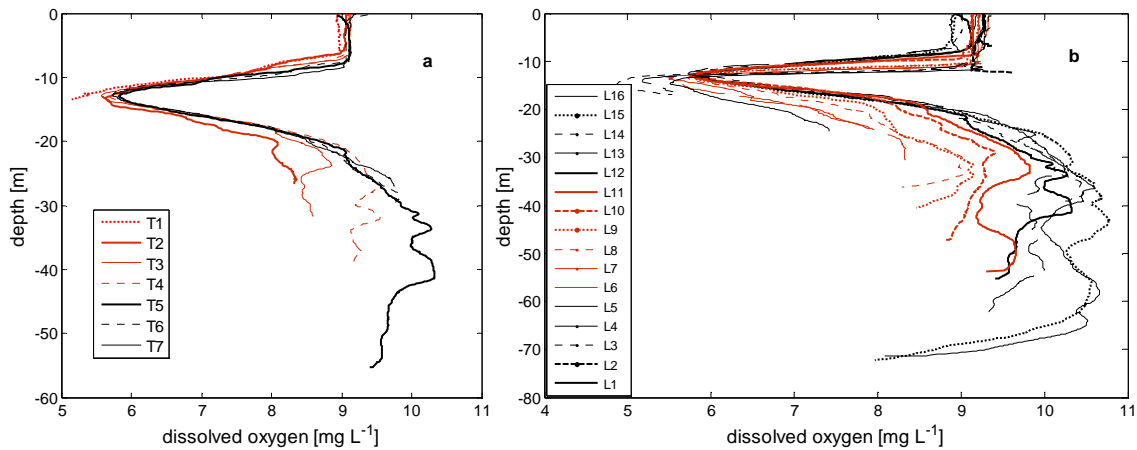


Figure 3: Profiles of oxygen on a transversal (a) and a longitudinal (b) transect measured on 10th September 2015. See Fig. 1 for locations of measuring stations.

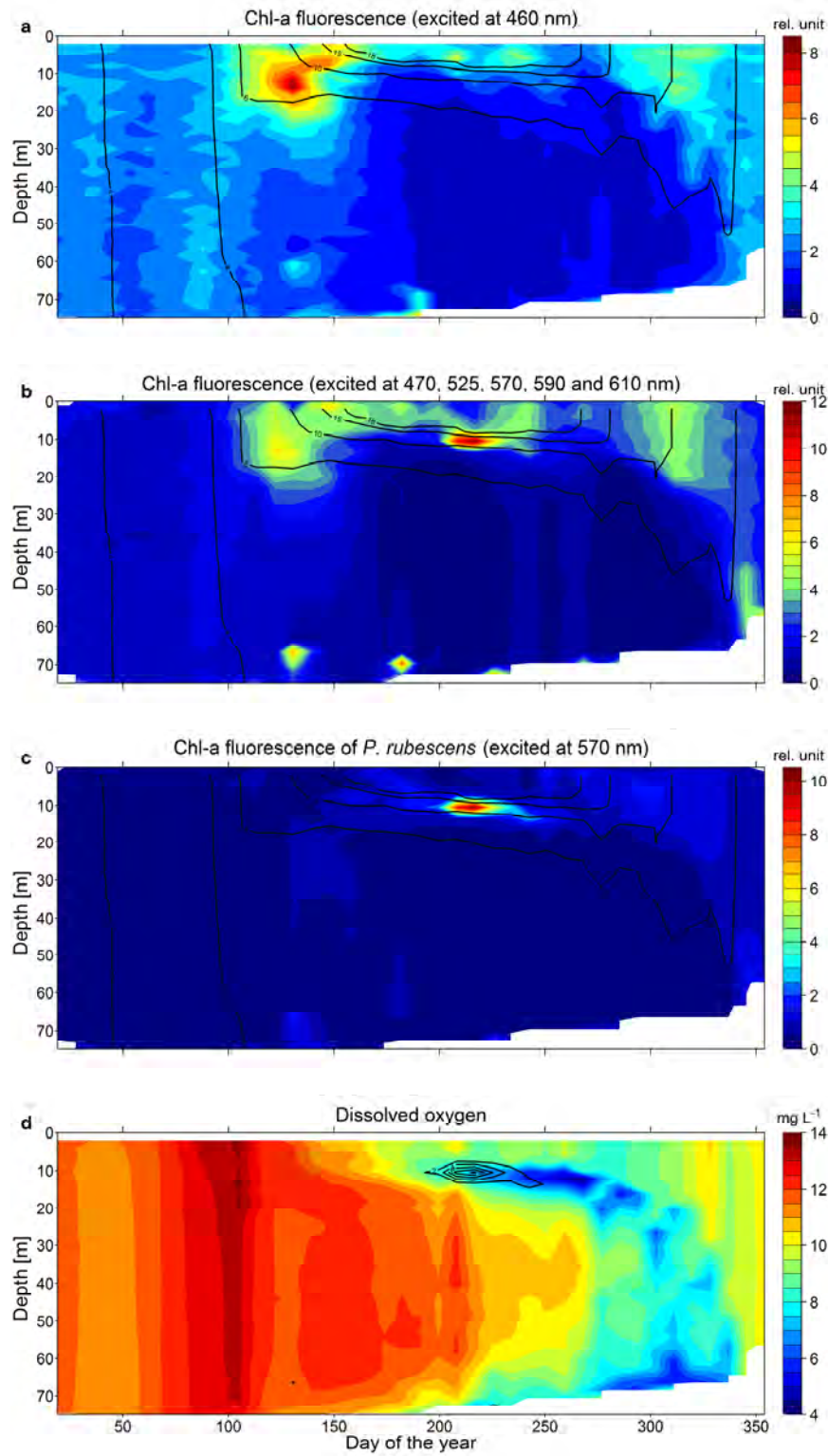


Figure 4: Seasonal and vertical development (depth vs. time) during the year 2016. Color contours of fortnightly profiles of (a) chlorophyll a fluorescence measured by CTD90M probe at excitation wavelength 460 nm, (b) summed chlorophyll a fluorescence measured by FluoroProbe at excitation wavelengths 470, 525, 570, 590 and 610 nm, (c) chlorophyll a fluorescence measured by FluoroProbe at excitation wavelength 570 nm (proxy for phycoerythrin-rich cyanobacteria and cryptophytes), (d) dissolved oxygen (mg L^{-1}). Contour lines indicate water temperature ($^{\circ}\text{C}$) (in Fig. 4a-c) or chlorophyll a fluorescence measured by FluoroProbe at excitation wavelength 570 nm (proxy for phycoerythrin-rich cyanobacteria and cryptophytes, in Fig. 4d).

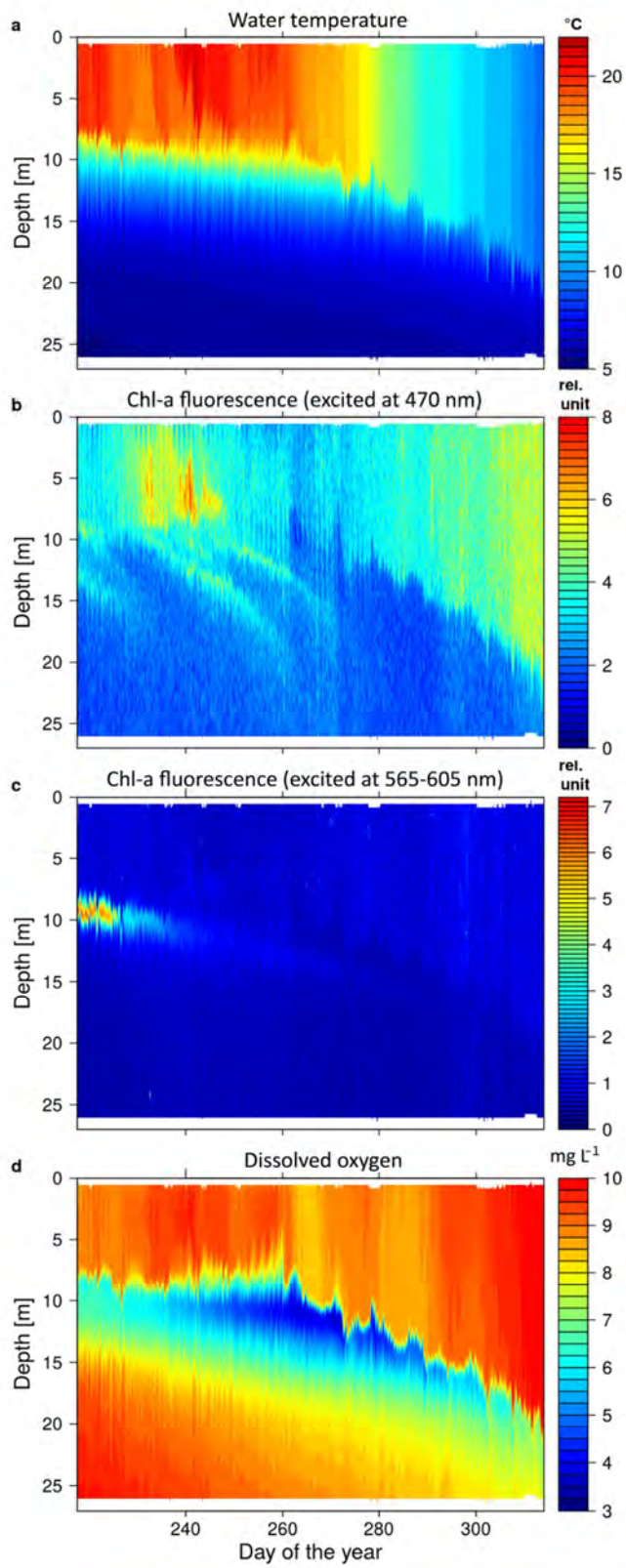


Figure 5: Seasonal and vertical development (depth vs. time) during the year 2016. Color contours display 3-hourly profiles of (a) water temperature (b) chlorophyll a fluorescence excited at 470 nm (c) chlorophyll a fluorescence excited through phycocyanin at 565-605 nm (d) dissolved oxygen.

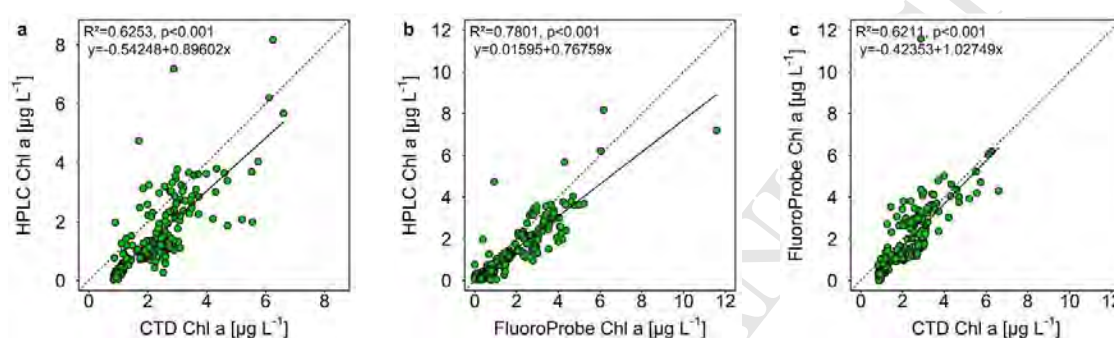


Figure 6: Relationship of different chlorophyll a quantification methods ($n=229$). Correlation between (a) HPLC and CTD90M probe, (b) HPLC and FluoroProbe, (c) FluoroProbe and CTD90M probe. The black line shows the regression line. The dashed line corresponds to the 1:1 relationship.

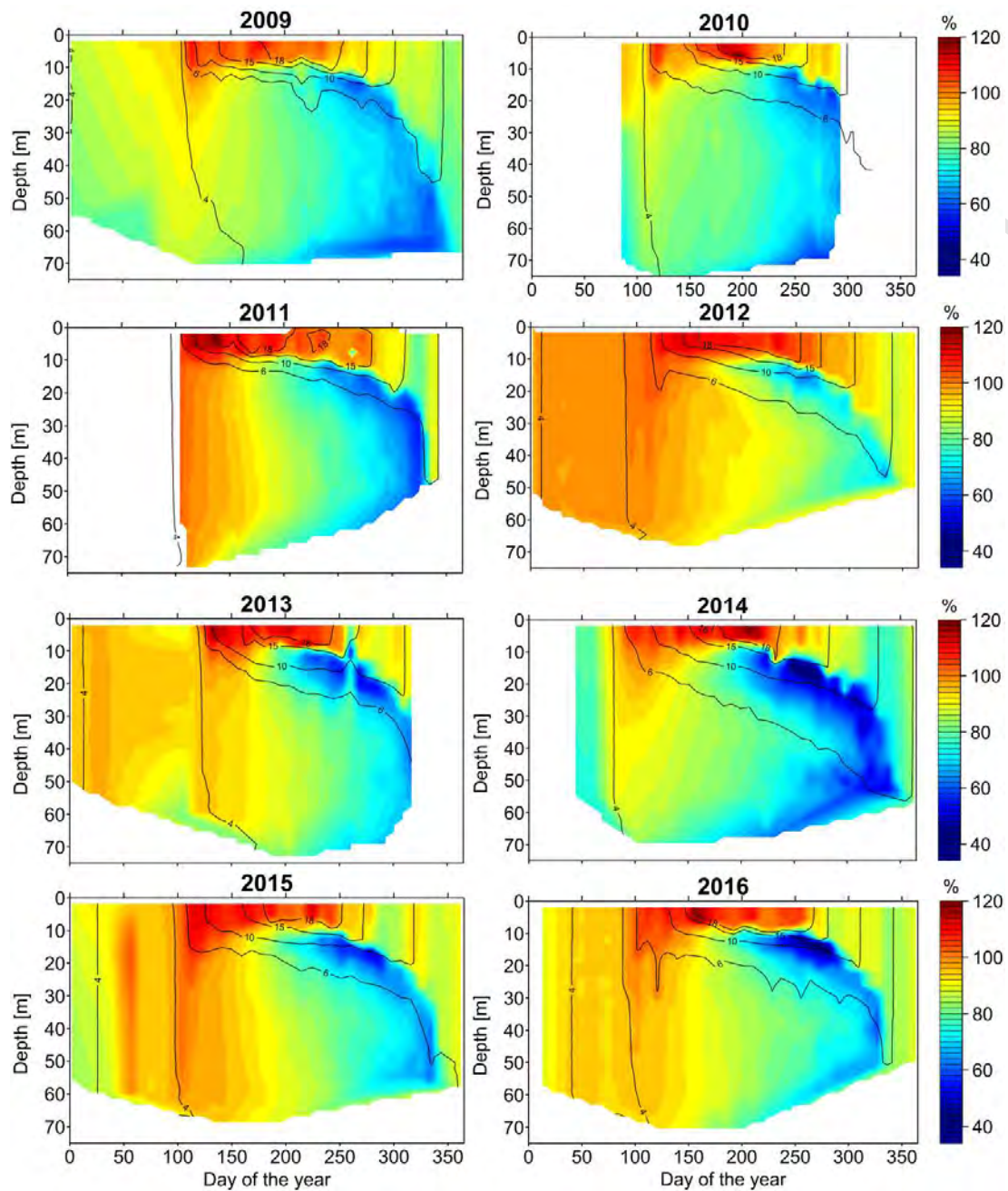


Fig. 7: Seasonal and vertical (depth vs. time) oxygen levels from 2009 to 2016. Color contours display oxygen profiles (oxygen saturation in %) and contour lines indicate water temperature ($^{\circ}\text{C}$).

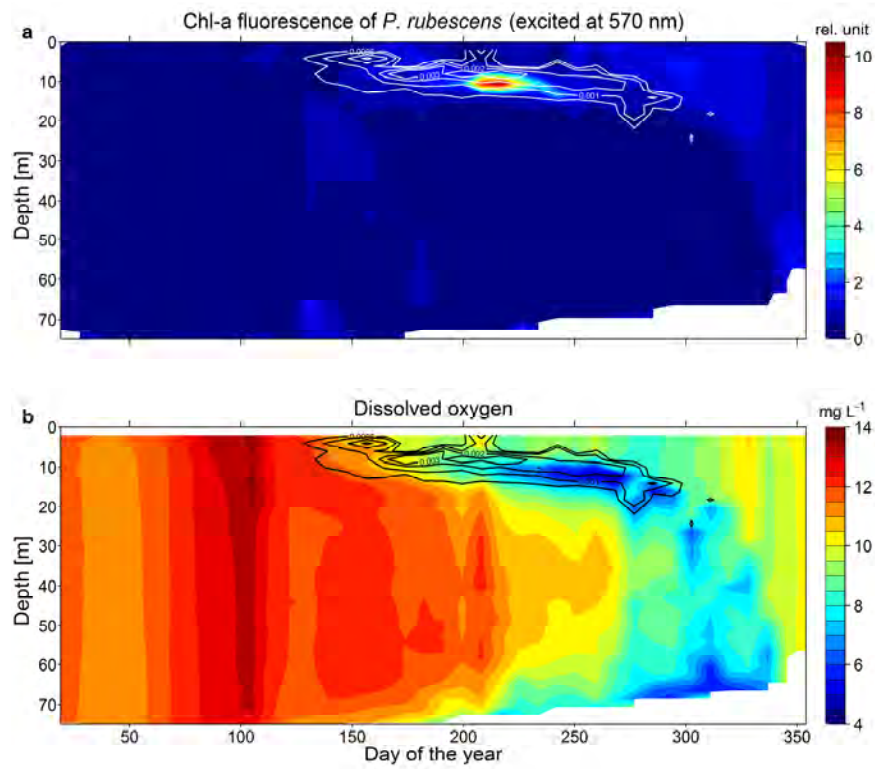


Fig. 8: Position within the stratification represented as contour lines of the squared buoyancy frequency N^2 [s⁻²] during 2016 of (a) chlorophyll a fluorescence measured by FluoroProbe at excitation wavelength 570 nm (proxy for phycoerythrin-rich cyanobacteria and cryptophytes) and (b) oxygen concentration.

Highlights

- A metalimnetic oxygen minimum (MOM) down to 40% saturation was observed in summer
- The MOM was not imported from the sediment at the side walls
- The MOM was a consequence of pelagic processes, such as respiration in the metalimnion
- We hypothesize that *Planktothrix rubescens* in the metalimnion caused the MOM